

Using mixed objects in the training of object-based image classifications

Hugo Costa, Giles M. Foody, and Doreen S. Boyd

School of Geography, University of Nottingham, Nottingham NG7 2RD, UK

Abstract

Image classification for thematic mapping is a very common application in remote sensing, which is sometimes realized through object-based image analysis. In these analyses, it is common for some of the objects to be mixed in their class composition and thus violate the commonly made assumption of object purity that is implicit in a conventional object-based image analysis. Mixed objects can be a problem throughout a classification analysis, but are particularly challenging in the training stage as they can result in degraded training statistics and act to reduce mapping accuracy. In this paper the potential of using mixed objects in training object-based image classifications is evaluated. Remotely sensed data were submitted to a series of segmentation analyses from which a range of under- to over-segmented outputs were intentionally produced. Training objects were then selected from the segmentation outputs, resulting in training data sets that varied in terms of size (i.e. number of objects) and proportion of mixed objects. These training data sets were then used with an artificial neural network and a generalized linear model, which can accommodate objects of mixed composition, to produce a series of land cover maps. The use of training statistics estimated based on both pure and mixed objects often increased classification accuracy by around 25% when compared with accuracies

20 obtained from the use of only pure objects in training. So rather than the mixed objects being a
21 problem, they can be an asset in classification and facilitate land cover mapping from remote
22 sensing. It is, therefore, desirable to recognize the nature of the objects and possibly
23 accommodate mixed objects directly in training. The results obtained here may also have
24 implications for the common practice of seeking an optimal segmentation output, and also act to
25 challenge the widespread view that object-based classification is superior to pixel-based
26 classification.

27 **Keywords: OBIA; mixed pixels; under-segmentation; over-segmentation; scale parameter**

28 **1. Introduction**

29 Information on the Earth's surface such as land cover and related environmental processes is of
30 great importance for a plethora of applications, for example for decision-making on issues related
31 to agriculture and food security (Fritz et al., 2013; Gardi et al., 2015), monitoring the distribution
32 of species (Martin et al., 2013; Tuanmu and Jetz, 2014), and modelling of the Earth's climate
33 (Luyssaert et al., 2014; Mahmood et al., 2014). For this reason, thematic mapping through a
34 classification analysis is a very common application of remote sensing. Over the years substantial
35 progress has been made in remote sensing-based mapping, and today there are many ways
36 through which a classification analysis can be conducted (Lu and Weng, 2007; Momeni et al.,
37 2016).

38 A key decision needed during a classification analysis is on which basic spatial unit to use.
39 Considerable use of the pixel, the basic spatial unit of a digital image, and per-pixel based

40 classification has been common for decades. However, grouping spatially connected pixels into
41 objects by means of an image segmentation analysis, and using the object as the basic spatial unit
42 has become very popular in recent years (Blaschke et al., 2014). The objects obtained from an
43 image segmentation analysis may, in principle, form a more suitable spatial unit than the pixel
44 for land cover mapping as they should relate to natural spatial units (e.g. fields) unlike pixels
45 which are artificial units defined more by the sensing system than the properties of the ground.
46 The use of objects comprising multiple pixels can also aid the calculation of potentially useful
47 discriminatory variables such as descriptors of image texture (Laliberte and Rango, 2009).

48 There are, however, fundamental issues and assumptions of classification that often appear to be
49 ignored or incompletely addressed in object-based image analyses. For example, it is common for
50 the objects produced from the segmentation analysis to be routinely and unquestioningly used as
51 if pure in the classification (e.g. Goodin et al., 2015; Shimabukuro et al., 2015; Uddin et al.,
52 2015). However, this is often not the case, mainly for two reasons. First, remotely sensed data
53 inevitably comprise a proportion of mixed pixels whatever the spatial resolution used (Addink et
54 al., 2012; Cracknell, 1998; Fisher, 1997), which cannot be accommodated by traditional image
55 segmentation. For example, Wu (2009) found that 40-50% of the pixels of an urban area
56 represented in multispectral IKONOS data (4 m resolution) were mixed. Second, image
57 segmentation often produces mixed objects as a result of under-segmentation error. This type of
58 error corresponds to situations such as the failure of the image segmentation analysis to define a
59 border splitting two land cover classes, thereby generating a single object containing more than
60 one class (Clinton et al., 2010).

61 Failure to satisfy the assumptions of classification can greatly degrade the quality of the land
62 cover map produced ultimately. In particular, the specific case of under-segmentation error (Gao
63 et al., 2011; Hirata and Takahashi, 2011; Wang et al., 2004) is a problem throughout the
64 classification process as mixed objects can degrade class training statistics, they cannot be
65 appropriately allocated to a single class, and any such allocation must to some extent be
66 erroneous (Heumann, 2011). Action is therefore needed to address the impact of these mixed
67 units. That said, deviation from the assumptions of classification can, however, sometimes be
68 made in each of the main stages of a classification analysis (e.g. Foody, 1999a). Specifically,
69 impure units can be accounted for in training (Eastman and Laney, 2002; Foody, 1997; Hansen,
70 2012; Zhang and Foody, 2001), class allocation (Dronova et al., 2011; Foody, 1996; Wang,
71 1990), and testing a classification (Binaghi et al., 1999; Foody, 1995; Stehman et al., 2007). For
72 example, van de Vlag and Stein (2007) generated objects based on remotely sensed data,
73 classified them using fuzzy decision trees, and produced fuzzy error matrices in accuracy
74 assessment. However, little research has been undertaken on the use of mixed units in training
75 object-based image classifications.

76 Typically, the objects used in training are assumed to be pure (i.e. contain a single class), but a
77 range of options are available if mixed objects are encountered. For example, the analyst could
78 seek to simply ignore the problem, act to exclude the mixed cases, or adopt procedures that can
79 accommodate the mixed nature of the units (Foody, 1999a, 1997). In object-based classification,
80 the presence of mixed objects in training is sometimes addressed beforehand by deliberately
81 favouring over-segmentation, that is, producing numerous small objects at the segmentation stage

82 (Boyden et al., 2013; Cánovas-García and Alonso-Sarría, 2015; Dronova et al., 2012; Van Coillie
83 et al., 2008). However, this approach may be sub-optimal (Dorren, 2003; Gao et al., 2011; Hirata
84 and Takahashi, 2011; Kim et al., 2009; Mishra and Crews, 2014) and is unlikely to remove all
85 impure objects (Zhou et al., 2009; Zhou and Troy, 2008). Another solution sometimes adopted is
86 the exclusion of mixed objects from the production of training statistics (Cai and Liu, 2013;
87 Dean and Smith, 2003; Dronova et al., 2011; Güttler et al., 2016). In this way, the mixed units,
88 which do not satisfy key assumptions of the analysis, are excluded so that the analysis can
89 proceed with suitable data. Excluding mixed objects has, however, the consequence that the size
90 of the training data sets will be reduced, and this could limit the quality of the resulting training
91 statistics. This issue is particularly relevant in object-based classifications as the pool of potential
92 training units is typically relatively small at the outset (Ma et al., 2015). Excluding mixed objects
93 from the pool of selectable objects can exacerbate the challenge of finding a sufficient number of
94 training objects (Mui et al., 2015; Wang et al., 2004).

95 Another issue to take into account while excluding mixed objects is the criteria according to
96 which an object should be considered as mixed. It is unclear whether an object containing a very
97 small fraction of pixels corresponding to a minority class should be excluded from training
98 because there is the chance of those minority pixels having a negligible impact on the training
99 statistics produced. For example, Cai and Liu (2013) excluded from training all objects whose
100 dominant class occupied less than 90% of the objects' area. The effect of issues such as threshold
101 selection have not been investigated in detail (Li et al., 2016) and is most likely to be dependent

102 on several factors, such as the remotely sensed data used and the land cover classes mixed
103 (Dronova et al., 2011).

104 The assumptions of a classification also impact on the way training data sets should be used. For
105 example, the training stage of a supervised classification should be designed in relation to the
106 chosen classifier as different algorithms use the data differently. Specifically, with a standard
107 statistical classifier, such as the maximum likelihood classification, it is important that each class
108 is described appropriately which often requires a relatively large and representative training
109 sample (Ediriwickrema and Khorram, 1997; Hagner and Reese, 2007; Paola and Schowengerdt,
110 1995; Richards and Kingsbury, 2014) while the use of a small sample of deliberately selected
111 extreme and atypical samples may be more suited to non-parametric classifiers, such as a
112 multilayer perceptron neural network, support vector machine, and classification tree (Foody,
113 1999b; Foody and Mathur, 2006; Hansen, 2012; Pal and Foody, 2012). Critically, the nature of
114 the data used in training a classification should be acknowledged and addressed.

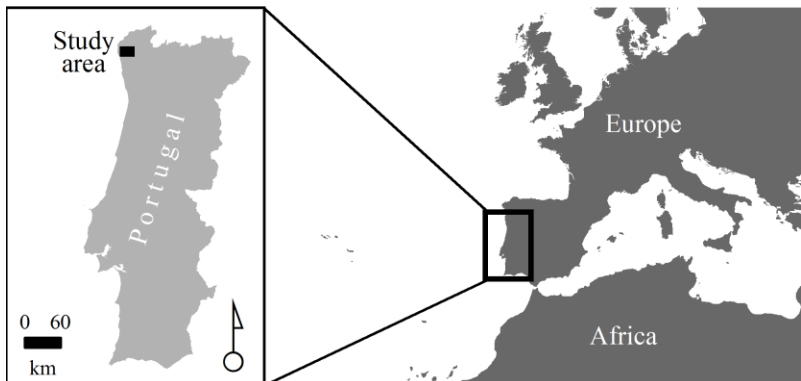
115 In this paper it is argued that it is not necessary, or even desirable, to exclude mixed objects from
116 training an object-based image classification. In particular, it is possible to turn the apparent
117 problem of mixed units into an asset, as with mixed pixels in per-pixel classification (Foody,
118 1997), recognizing that each individual mixed unit can be a source of training data on more than
119 one class, and that mixed units can be used in training. Here, the potential of using mixed objects
120 in training an object-based image classification is evaluated. A series of image segmentation
121 analyses were undertaken from which training objects were selected, resulting in training data

122 sets that varied in terms of size and proportion of mixed objects. The mixed objects generated at
123 the segmentation stage and encountered at the training stage are included in the set of objects
124 used to estimate training statistics, and the classification outputs produced by two classifiers are
125 evaluated in relation to a conventional analysis using only pure objects. Thus, the work sets out
126 to test the hypothesis that mixed objects may be used in the training of object-based image
127 classifications to increase the accuracy with which land cover may be mapped from remotely
128 sensed data.

129 **2. Materials and methods**

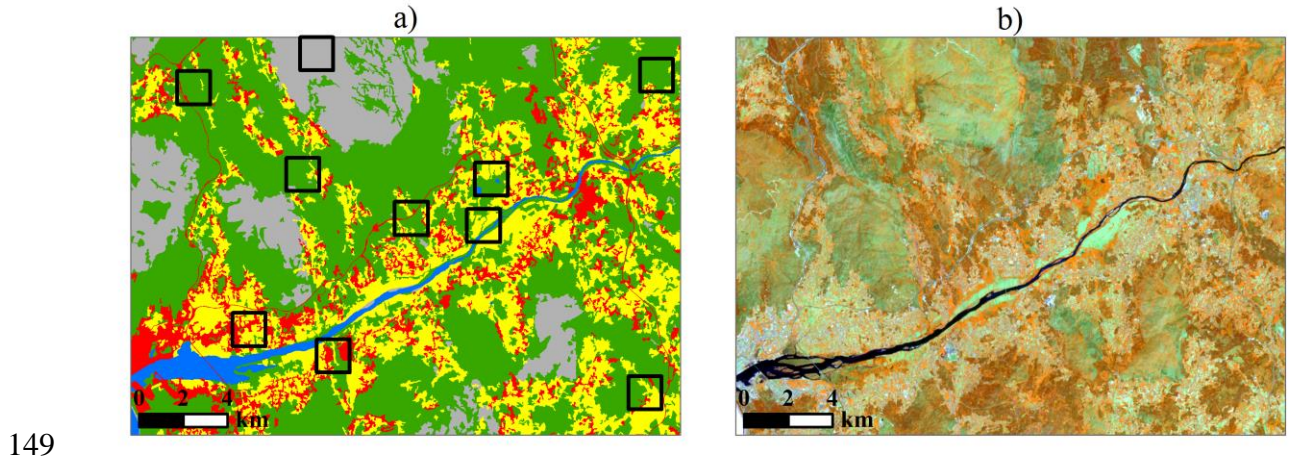
130 **2.1 Study area and data sets**

131 The analyses focused on a test site of approximately 45,000 ha in northern Portugal (Figure 1).
132 The area corresponds to the downstream part of river Lima where the city of Viana do Castelo is
133 settled. A diverse range of land cover types are present in the study area, and five land cover
134 classes were defined: Artificial surfaces, Agricultural areas, Forest and semi-natural areas, Open
135 spaces with little or no vegetation, and Wetlands and water bodies.



136
137 Figure 1. Location of the study area.

138 A Portuguese map, “Carta de Ocupação do Solo” of 2007 (COS2007), was used as reference data
139 set (Figure 2a) in training and testing the object-based classifications. This map was produced by
140 the Portuguese mapping agency (Direção-Geral do Território) through visual interpretation of
141 aerial imagery and use of auxiliary data such as field work and the national forest inventory. Land
142 cover is represented according to a nomenclature similar to that used in this study in the third of a
143 total of five hierarchical thematic levels used to map land cover with a minimum mapping unit of
144 1 ha (Caetano et al., 2010). As a guide to the thematic accuracy of the map, the overall accuracy
145 is $96.82 \pm 1.01\%$ at the 95% confidence level for the thematic detail used in this article, 5 classes,
146 and the producer’s accuracy for each of the classes is $>92\%$. This map provides the most accurate
147 and detailed representation of the land cover that is available for the region and hence is suitable
148 as reference data in the production and assessment of optimal image classifications in this study.



150 Figure 2. Data sets used: a) reference land cover map, COS2007, representing Artificial surfaces in red,
151 Agricultural areas in yellow, Forest and semi natural areas in green, Open spaces with little or no
152 vegetation in grey, and Wetlands and water bodies in blue; the square areas outlined in black are the
153 training areas randomly located for the estimation of object-based training statistics. b) LISS-III image
154 collected in Summer of 2006; RGB composition of data acquired in the near infrared, short wave infrared
155 and red bands respectively.

156 Two images acquired during Spring and Summer of 2006 (Figure 2b) by the Linear Imaging Self
157 Scanning Sensor (LISS-III) onboard IRS-P6 (also known as ResourceSat-1) were used. These
158 two images are part of the IMAGE2006 European coverages provided by the European Space
159 Agency (Müller et al., 2009). LISS-III is a multi-spectral camera operating in four spectral bands
160 (green, red, near infrared, and short wave infrared) with a spatial resolution of 23 m in each. The
161 two LISS-III images were orthorectified and resampled to 25 m spatial resolution using an
162 SRTM-based digital elevation model (Müller et al., 2009). The four bands of the two images
163 were stacked and thus formed an eight waveband data set.

164 **2.2 Image segmentation**

165 The LISS-III data were segmented using the multiresolution algorithm implemented in GeoDMA
166 software (Körting et al., 2013), version 0.2.1, which is based on the popular algorithm of Baatz
167 and Schäpe (2000). This is a region-based algorithm that uses spectral and shape properties of the
168 objects being generated. Colour and shape parameters range within the interval 0-100 and are
169 inversely proportional (i.e. colour=100-shape). In addition, the parameter shape depends on two
170 other parameters, compactness and smoothness, also ranging within the interval 0-100 and
171 inversely proportional. Finally, scale is a threshold of heterogeneity allowed within objects as

172 regard colour, and shape properties. Essentially, the larger the scale parameter value the larger
173 the heterogeneity allowed within objects, thus making larger and fewer objects (Körting et al.,
174 2013).

175 The scale, colour, and shape parameter values are the most influential parameters (Luo et al.,
176 2015) and were varied to obtain a series of different segmentations. First, five values were
177 defined for the parameter colour, covering the entire range of possible values for this parameter:
178 1, 25, 50, 75, and 99. The importance of the spectral properties of the objects is positively related
179 to the magnitude of the colour parameter. For simplicity, the parameter shape is not discussed
180 hereafter as its value is automatically known for a given value of parameter colour. Then, for
181 each of the five colour parameter values defined, the scale parameter was varied greatly as this is
182 the most influential parameter (Luo et al., 2015). Specifically, eight values were defined from 10
183 to 80 in steps of 10. As a result, 40 segmentation outputs were obtained, ranging from over-
184 segmented results mostly composed of small and possibly pure objects to under-segmented
185 results mostly composed of large and possibly mixed objects. For the purposes of this paper an
186 object was taken to be pure if more than 90% of its area was covered with a single class, similar
187 to Cai and Liu (2013).

188 **2.3 Training**

189 A fraction of the study area was randomly selected for training purposes. Specifically, ten 225 ha
190 square areas were selected randomly to provide training data. As a result, a total of 2250 ha,
191 which is ~5% of the study area (Figure 2a), was available for training purposes. The training

192 areas were intentionally defined as being small relative to the study area to simulate the limited
 193 availability of reference data that are typical of real-world applications. The objects of each of the
 194 segmentation outputs that intersected the training areas were selected for the production of
 195 training statistics. The objects generated via image segmentation are commonly used for
 196 estimating training statistics (e.g. Goodin et al., 2015). Thus, while the same geographical area
 197 was used in training each classification the set of objects used varied between the segmentation
 198 outputs. As a result, the training statistics varied between segmentation settings. In all cases,
 199 however, the representation of the land cover classes was constant and proportional to their
 200 abundance (Table 1) as the training areas defined were constant and randomly located.

201 Table 1. Proportion of area of the land cover classes mapped in the reference COS2007 land cover map
 202 in the training areas defined. The relative proportion of the classes is common to all training statistics
 203 estimated from the segmentation settings used.

Land cover class	Proportion of area (%)
Artificial surfaces	9.87
Agricultural areas	25.99
Forest and semi-natural areas	52.26
Open spaces with little or no vegetation	10.35
Wetlands and water bodies	1.53

204

205 The mean and standard deviation of the digital numbers of each object in the eight LISS-III
206 spectral bands were used as training statistics, resulting in a total of 16 discriminating variables.
207 The training objects were assigned reference class labels extracted from the COS2007 land cover
208 map. The proportion of the area that each class occupied in a training object was estimated,
209 ranging from 0.0 if the class was absent to the maximum value of 1.0 if the object was pure, with
210 intermediate values for at least two classes if the object was of mixed class composition.

211 The remotely sensed data were classified using each of the segmentation outputs produced. Two
212 scenarios were followed. First, following the traditional procedure of using only pure objects at
213 the training stage. Specifically, each object intercepting the training areas was taken as pure and
214 hence allowed to be a training object only for the class with which had the maximum
215 membership based on the proportion of class area, which had to be superior to 90% (otherwise
216 they were excluded from training). Second, all of the training objects, even if some were mixed,
217 were used. The fractional coverage of the classes found in the objects was used as a measure of
218 class membership, and training objects were allowed multiple and partial membership.

219 Because mixed objects were not excluded from training in the mixed training strategy, the size of
220 the mixed training data sets was typically larger than when only pure objects were used. Since the
221 size of the training set may impact the classification accuracy (Ma et al., 2015; Millard and
222 Richardson, 2015) a series of analyses in which training set size was constant was also
223 undertaken. For this additional analyses, reduced versions of the mixed training data sets were
224 generated, with the size of the mixed data sets decreased to equal the size of the pure training

225 data sets. The reduction of the size of the mixed training data sets was achieved by excluding
226 randomly selected objects. Since the mixed training data sets may comprise both pure and mixed
227 objects, this approach means that all objects, pure and mixed, had the same probability of being
228 excluded. This allowed the size of the training data sets to be reduced without changing
229 substantially the inherent ratio of pure to mixed objects. As the random exclusion of objects can
230 result in numerous and different training data sets each of which with a potential different impact
231 on the results, three reduced mixed training data sets were produced from each mixed training
232 data set.

233 A series of classifications of the remotely sensed data using all 40 segmentation outputs was
234 produced. With each segmentation output, classifications were produced that were trained using
235 (i) pure training data sets, (ii) mixed training data sets, and (iii) the reduced (to same size as pure)
236 training data sets.

237 **2.4 Classification**

238 In all analyses, multinomial regression models fitted by means of an artificial neural network
239 with no hidden layer (Venables and Ripley, 2002) and a generalized linear model via penalized
240 maximum likelihood (Friedman et al., 2010) were used for classification. These classifiers are
241 available in the R programming language (R Core Team, 2016) from the packages ‘nnet’ and
242 ‘glmnet’ respectively. Both classifiers allow fractional composition of the objects to be used in
243 training in a manner similar to that explained in Foody (1997) for per-pixel classification.

244 The output of the classifiers is soft, indicating the probability of an object belonging to each class
245 (Friedman et al., 2010; Venables and Ripley, 2002). However, traditional hard land cover maps
246 were estimated by allocating each object the label of the class with which it had the greatest
247 probability of membership. Although it may be beneficial to address the potential mixed nature
248 of the objects at the class allocation stage, hard classification was adopted to confine the focus of
249 the paper to the training stage. Each segmented image was thus used to produce hard land cover
250 maps based on different training strategies: pure, mixed, and reduced mixed.

251 **2.5 Accuracy assessment**

252 The thematic accuracy of each classification produced was assessed. Confusion matrices
253 comparing the land cover maps produced and the reference COS2007 land cover map were
254 constructed through an operation of spatial intersection of the two data layers. Thus, instead of
255 using a sample to estimate classification accuracy, the entire study area was used to assess the
256 accuracy with which each of the 40 segmentation outputs produced was classified. Note,
257 however, that the area associated with training (Figure 2a) was not used for accuracy assessment
258 because that would artificially increase classification accuracy. Classification accuracy was
259 expressed in terms of proportion of area correctly classified. Because the entire study area was
260 used to estimate proportions of area correctly and incorrectly classified, the issues of selecting
261 either pixels or objects as sampling units and producing estimates of accuracy which holds
262 statistical uncertainty do not arise.

263 The accuracy of the 40 segmentation outputs generated was also assessed to provide a measure of
264 under- and over-segmentation error, which is useful for analysis of the results. The method
265 developed by Möller et al. (2013) and slightly refined by Costa et al. (2015) was used. This
266 method belongs to a popular family of methods widely known as empirical discrepancy or
267 supervised methods (Clinton et al., 2010; Zhang, 1996), and essentially compares the image
268 segmentation output under evaluation to a reference data set (e.g. land cover map) to measure the
269 geometric match between the objects that form them. Möller et al.'s (2013) method includes
270 typical area-based and position-based metrics such as the ratio of overlapping area among
271 generated and reference objects and the distance between the objects' centroid (Clinton et al.,
272 2010; Whiteside et al., 2014) to detected and measure under- and over-segmentation error
273 separately. The metrics are the basis for finding an optimal segmentation output that offsets the
274 two types of error while informing on which type predominates when unbalanced, which is
275 useful for this study. A summary of the segmentation accuracy is provided by metric M^g which
276 measures the strength and type of segmentation error. Negative M^g values indicate that under-
277 segmentation error dominates while positive M^g values represent the opposite case in which
278 over-segmentation error dominates. Therefore, $M^g \sim 0$ is considered indicative of optimal
279 segmentation accuracy as both types of error are balanced (Möller et al., 2013). The reference
280 data set used was the set of polygons of the COS2007 land cover map over the training areas
281 defined. Thus, it was possible to determine whether the training data sets used were over-
282 segmented, under-segmented, or balanced.

283

3. Results

284

The 40 segmentation outputs generated varied greatly in nature from over- to under-segmented,

285

as expected, and two examples are shown in Figure 3 to highlight the different sets of objects

286

obtained. The geometric accuracy of the objects that intersected the training areas, and hence

287

used for training, was assessed, and the results are presented in Figure 4. Small values of the

288

parameter scale produced over-segmented training objects ($M^g > 0$) while large scale values

289

yielded under-segmented outputs ($M^g < 0$). For intermediate scale values, the type and magnitude

290

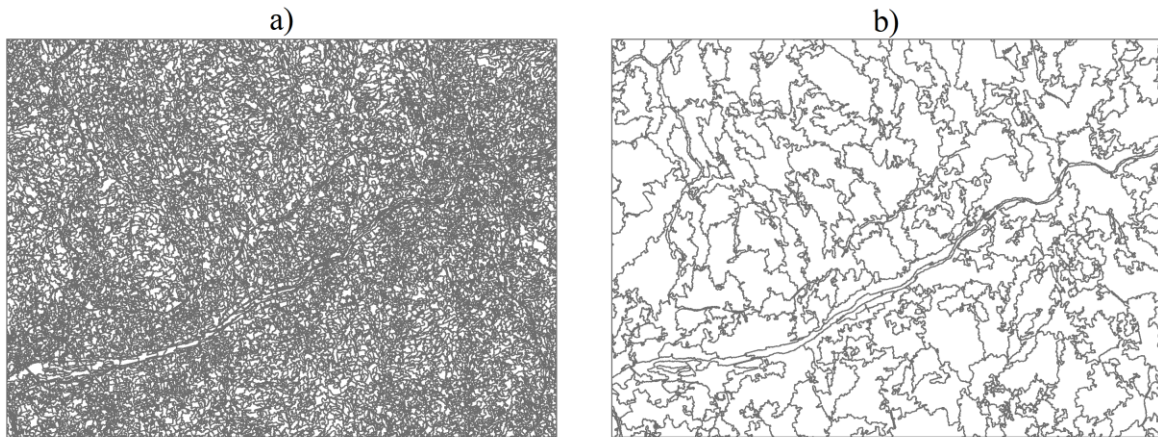
of segmentation error became less evident. According to the Costa et al.'s (2015) adaptation of

291

Möller et al.'s (2013) method, the scale value of 10, 30, 40, 50, and 70 were close to being

292

optimal when the parameter colour was set at 1, 25, 50, 75, and 99, respectively, as $M^g \sim 0$.

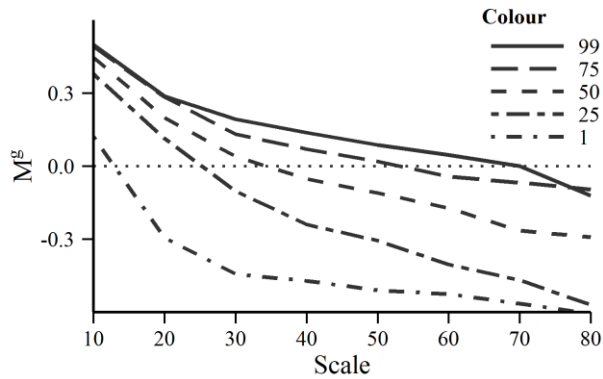


293

294 Figure 3. Segmentation results: a) Segmentation output produced with colour=75 and scale=10. b)

295

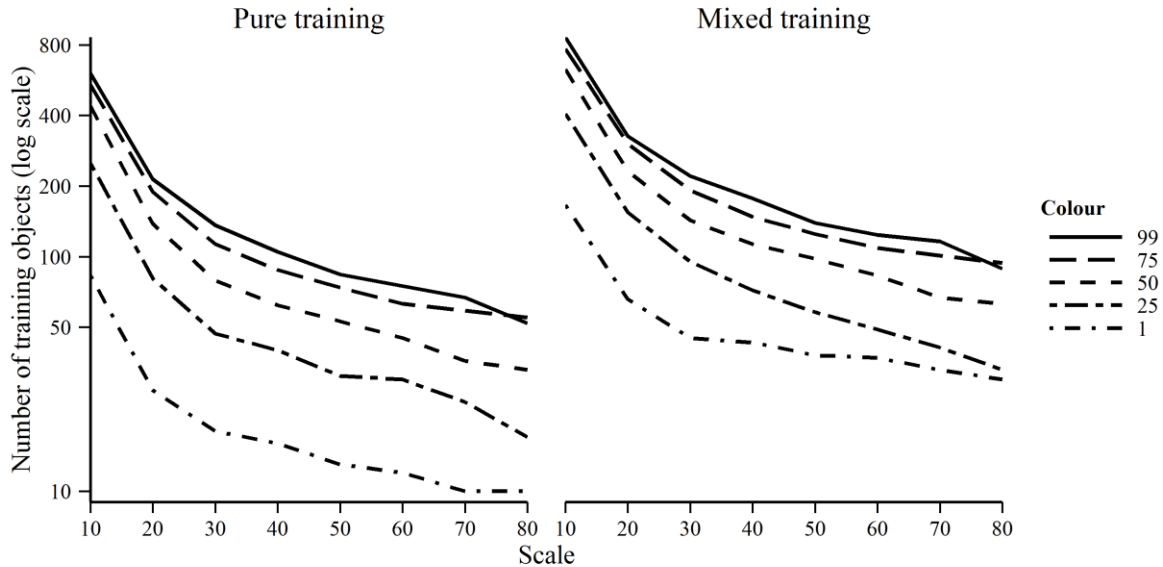
Segmentation output produced with colour=75 and scale=80.



296
 297 Figure 4. Segmentation accuracy based on Costa et al.'s (2015) adaptation of Möller et al.'s (2013)
 298 method. Dotted horizontal line corresponds to optimal accuracy.

299 The range of segmentation outputs generated resulted in training data sets of varying sizes
 300 (Figure 5). The number of training objects was large when over-segmentation was large (i.e.
 301 small values of parameter scale), and decreased as the level of under-segmentation increased. For
 302 example, when the parameter scale was set at 10 and 80, the training data sets generated
 303 comprised >430 and <100 training objects respectively. For a same value of parameter scale,
 304 larger training data sets were obtained when parameter colour was large. In all cases, some
 305 objects were mixed and hence the number of pure objects generated by a segmentation analysis
 306 was always less than the total number of objects generated. As such more objects were available
 307 for training when mixed rather than only pure objects were allowed. Specifically, 30-70% of the
 308 total number of the training objects was excluded when only pure objects were permitted in
 309 training. For example, the apparently near optimal segmentation output generated using
 310 colour=50 and scale=40 comprised 113 objects of which only 62 were pure (Figure 5). Thus, 51
 311 objects (45% of the total) were of mixed class composition and hence excluded when only pure

312 objects were allowed in training using an apparently near optimal segmentation. Mixed objects
 313 should, therefore, be expected to occur and even be common in object-based analyses.



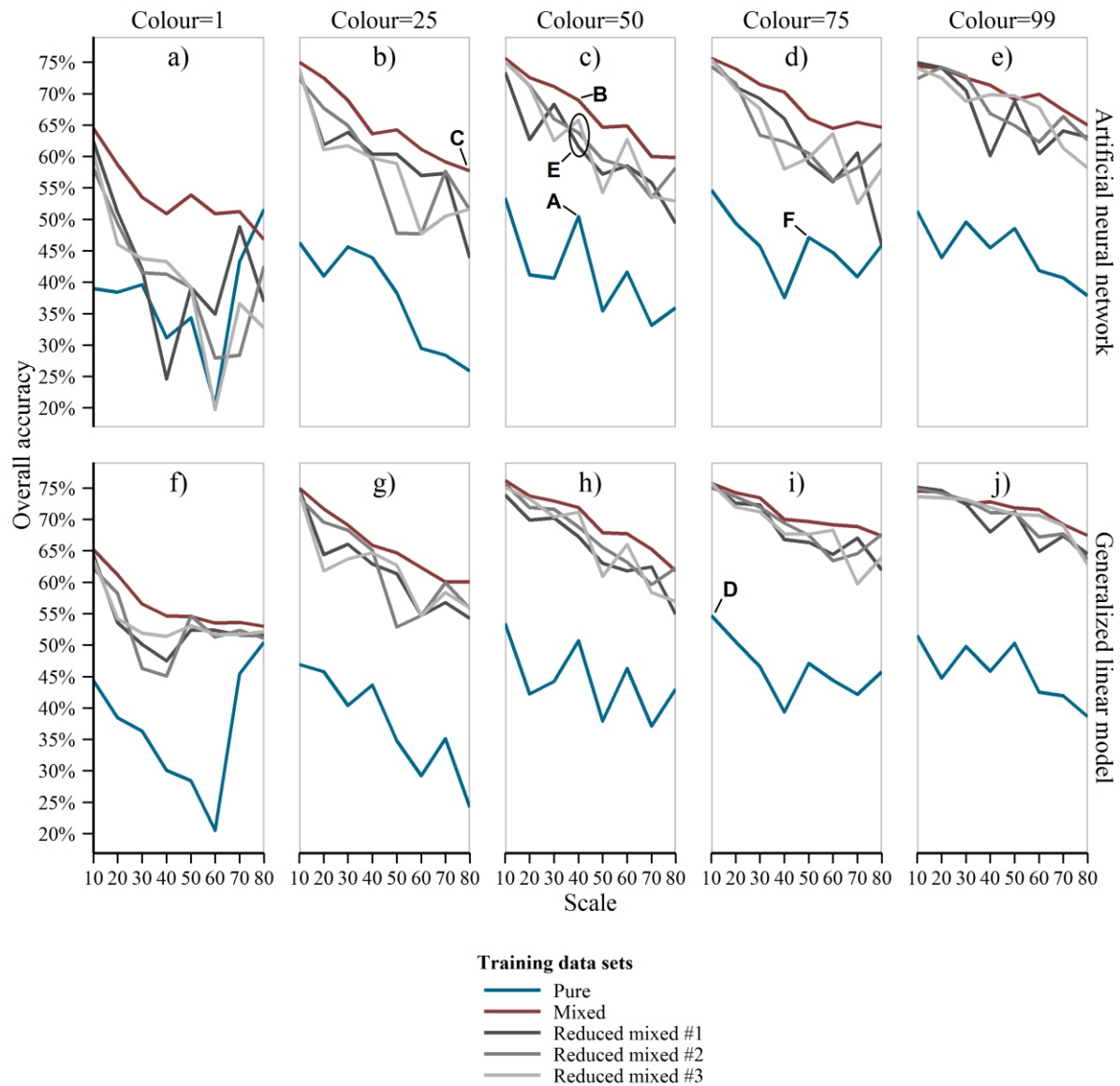
314
 315 Figure 5. Size of training data sets.

316 The nature of the training data sets had a considerable impact on classification accuracy
 317 regardless of the classifier used. In general, the generalized linear model enabled classification to
 318 reach larger accuracy than the artificial neural network due to the regularization procedure of the
 319 former, but the results are consistent between them while excluding or allowing mixed objects in
 320 training. Critically, the magnitude of classification accuracy was consistently smaller for the
 321 classifications that excluded mixed objects in training relative to that which allowed mixed
 322 objects (Figure 6). For example, using the artificial neural network and segmentation output
 323 colour=50 and scale=40, the classification accuracy was 50.4 and 69.0% when the pure and
 324 mixed training data sets were used respectively (points A and B in Figure 6c; Figure 7a,b). The

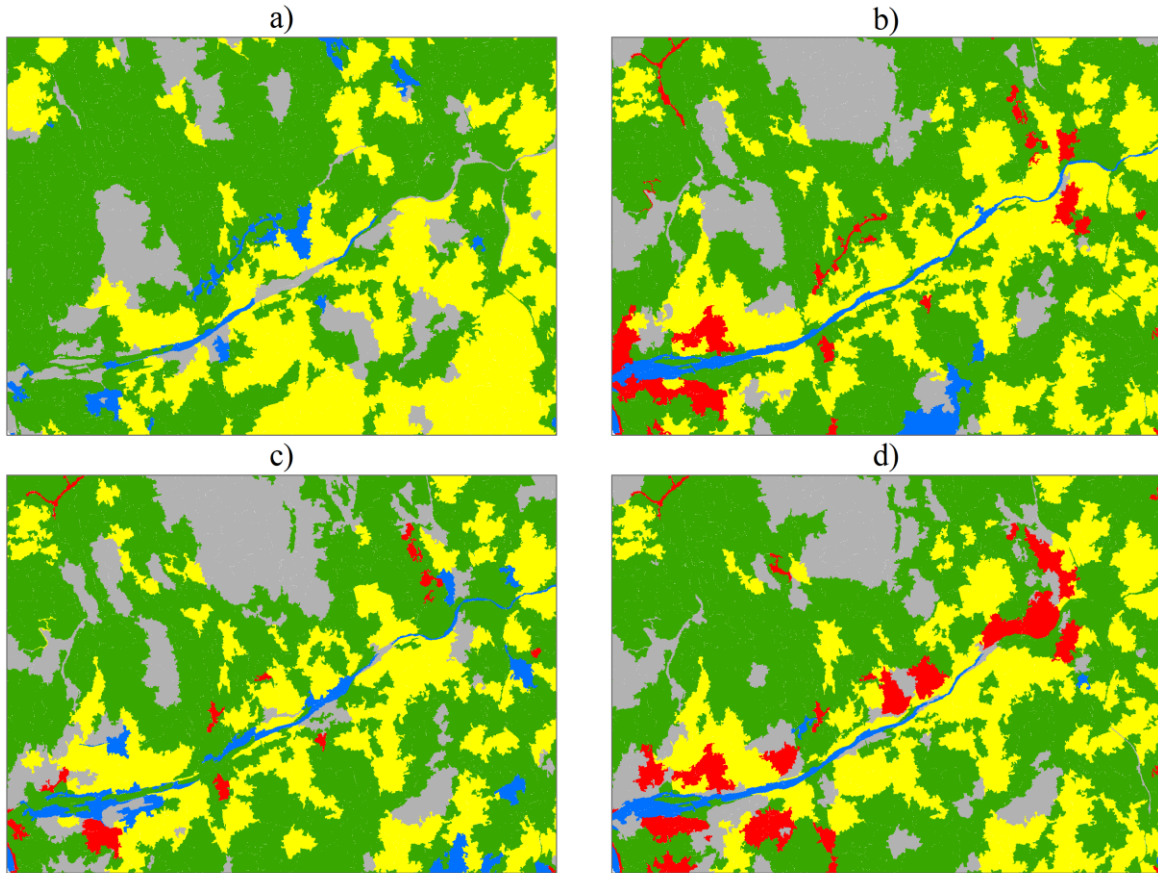
325 differences observed in terms of classification accuracy were so substantial that the smallest
326 accuracy achieved with the use of the mixed training data sets (57.7%; point C in Figure 6b,
327 using 33 training objects) was larger than the largest accuracy achieved with the use of only pure
328 training data (54.7%; point D in Figure 6i, using 540 training objects) if the results obtained with
329 colour=1 (Figure 6b and Figure 6f) are ignored. The minimum value of parameter colour was
330 associated with somewhat atypical results. For example, the segmentation settings defined by
331 colour=1 and scale=80 are associated with an increase in classification accuracy when trained
332 with only pure objects, but the quality of the land cover maps is very small. Specifically, virtually
333 the entire study area was classified as Forest and semi-natural areas class, and hence the
334 classification accuracy tends to converge with the proportion of the study area covered by that
335 class (~50%). The results obtained using colour=1 were caused mainly by the extremely small
336 consideration of spectral information while generating the objects, and thereby relatively large
337 values for the parameter colour are commonly used. The results obtained with this particular
338 value of parameter colour are not referred or discussed hereafter for simplicity.

339 The reduced mixed training data sets also afforded larger classification accuracy than the pure
340 training data sets. For example, the reduced mixed training data sets used to classify the
341 segmentation output produced using colour=50 and scale=40 were enough for the accuracy of the
342 artificial neural network to reach 61.6, 63.8, and 65.8% (points E in Figure 6c, Figure 7c,d),
343 substantially more than with the use of pure training data (50.4%; point A in Figure 6c). There
344 are a few cases in which the reduced mixed training data sets produced slightly larger
345 classification accuracy than the full mixed training data sets, particularly when parameters colour

346 and scale were large and small respectively (Figure 6e and Figure 5j). Thus, the difference in the
347 accuracy achieved with the use of pure and mixed training sets is not simply an issue of training
348 set size; mixed objects appear useful to produce valuable discriminatory information. The ability
349 to increase classification accuracy through the use of mixed training objects should help the
350 production of land cover maps that meet user needs and exceed appropriate target accuracy
351 values (Foody, 2008). The key issue in relation to the hypothesis being tested in this article,
352 however, is that the use of mixed objects can substantially increase classification accuracy
353 relative to that achieved when only pure training objects are used. The difference in accuracy
354 arising from the use of mixed and pure training sets varied with the specific parameter settings of
355 the classifications, but was typically large. Specifically, difference in accuracy between
356 classifications trained using pure and mixed training sets was up to 36% but typically in the order
357 of 20% (Figure 6).



358
 359 Figure 6. Classification accuracy as a function of the parameter scale with parameter colour set at 1, 25,
 360 50, 75, and 99. The results obtained using the three reduced versions of the mixed training data sets are
 361 identified as #1, #2, and #3. Panel a) to e) and f) to j) refer to the artificial neural network and
 362 generalized linear model respectively.



363
 364 Figure 7. Land cover maps obtained using the segmentation output produced with colour=50 and
 365 scale=40, the artificial neural network, and different training strategies. a) Pure training (accuracy:
 366 50.4%). b) Mixed training (accuracy: 69.0%). c) Mixed training with reduced samples #1 (accuracy:
 367 61.5%). d) Mixed training with reduced samples #3 (accuracy: 65.8%). Colour legend as in Figure 2.

368 Beyond the evident difference between the classifications generated with pure and mixed, even if
 369 reduced, training data, there is a clear positive trend in classification accuracy with over-
 370 segmentation. The largest overall accuracies were reached using scale=10 regardless of the
 371 colour parameter values defined (25, 50, 75, or 99) and training strategy used (pure or mixed).
 372 However, there were differences in the way classification accuracy varied as a function of the
 373 parameter scale. Classification accuracy decreased continuously with increasing scale values

374 when the entire mixed training data sets were used (smooth decreasing red lines in Figure 6);
375 classification accuracy decreased variably when the reduced mixed training data sets were used
376 (fluctuating decreasing grey lines in Figure 6), which is likely due to the random exclusion of
377 specific training objects – objects with more or less impact on the training statistics could be
378 excluded; finally, classification accuracy also tended to decrease as a function of the parameter
379 scale when the pure training data sets were used, but marked variations are visible in Figure 6
380 (fluctuating blue lines). Overall accuracy sometimes peaked locally around the regions indicated
381 as being close to balanced segmentation errors ($M^g \sim 0$), for example when the colour parameter
382 was set at 50 and 75 and the artificial neural network was used (point A in Figure 6c and point F
383 in Figure 6d). The local peaks around the regions indicated as being close to balanced
384 segmentation errors agree with numerous studies reporting that segmentation results neither over-
385 nor under-segmented are associated with land cover maps of larger thematic accuracy which have
386 been produced via an image classification analysis trained with pure data (Dorren, 2003; Gao et
387 al., 2011; Hirata and Takahashi, 2011; Kim et al., 2009; Kim and Warner, 2011; Mishra and
388 Crews, 2014).

389 **4. Discussion**

390 Object-based classification of LISS-III data benefited from allowing training data sets to include
391 mixed objects. An important advantage of mixed training is the opportunity to use relatively
392 large training data sets since there is no need to exclude mixed objects. Furthermore, mixed
393 objects allow efficiency as they give information on more than one class. It is well-known that
394 the size of a training sample often positively influences classification accuracy (Ma et al., 2015;

395 Millard and Richardson, 2015). However, the size of the training data sets is not the only factor
396 explaining the results obtained. When the parameter scale was set at small values, the pure
397 training data sets were large, but the classification accuracy continued to be relatively small. On
398 the contrary, mixed training afforded larger classification accuracy than pure training, even when
399 the mixed training data sets were small. Indeed, the results obtained from the reduced mixed
400 training data sets are closer to those obtained from the full mixed rather than the pure training
401 data sets. Note that the difference in classification accuracy achieved with full and reduced mixed
402 training data sets shrank with an increase in over-segmentation (Figure 6). This suggests that the
403 size of the training data sets produced from extremely over-segmented outputs is not entirely
404 needed, that is a smaller number of training objects may be sufficient to produce similar
405 classification results as long as mixed objects are allowed in training.

406 Mixed objects provide useful discriminatory information, and this may be the main advantage of
407 allowing mixed objects in training. Specifically, a representative sample of the objects generated
408 is used, which includes objects of mixed in addition to pure class composition. Thus, classifiers
409 can learn that the spectral properties of the objects may stem from the spectral signature of
410 thematic classes as well as their mixture. Mixed units must convey information on more than one
411 class and also will, in feature space, tend to lie between the classes involved. As a result of the
412 latter the mixed units may be expected to lie close to the classification hyperplane that separates
413 the classes. Mixed units, therefore, may have the potential to aid class separation, the central aim
414 of a classification analysis. This potential can be exploited when the classifier can directly
415 accommodate mixed responses in training and uses the training cases, rather than summary

416 statistics, directly (Foody, 1999b; Foody and Mathur, 2006). Focus on separability rather than
417 description of classes has been focus of innovative learning methods in recent years, such as
418 active learning with mixed spectral responses (Samat et al., 2016). This may be especially
419 relevant for classification as mixed objects may be common in an image segmentation output.

420 The use of mixed units is not without challenges. For example, due to intra-class spectral
421 variation it is possible for units of slightly different thematic composition to have the exact same
422 spectral response. However, the general trend is for mixed units to lie between the relevant
423 classes in feature space. The exact position in feature space is a function of the mixing. A unit
424 dominated by one class might be expected to lie relatively close to that class and still be distant
425 from the other(s) involved while one of more equal mixing lies more centrally between the
426 classes; exact details will depend on the specific classes and details (Foody, 2000; Hill et al.,
427 2007; Lee and Lathrop, 2006; Zhu et al., 2013). Another difference between the pure and mixed
428 training strategies relates to the fluctuating classification accuracy observed across the range of
429 segmentation levels used. The accuracy of the classifications that used only pure training data
430 was highly variable as a function of the parameter scale. These results were possibly caused by
431 the imbalanced number of training objects per class (Table 1) and the relatively small size of the
432 pure training data sets (Ma et al., 2015). Imbalanced training sets and the limited spectral
433 resolution of the data used may have set limits to the achievable accuracy and larger accuracy
434 could potentially be achieved with a larger, more balanced, training set and hyperspectral data
435 (Carrão et al., 2008). On the contrary, by setting parameter colour at relatively large values

436 benefited classification accuracy irrespective of the training strategy followed because the
437 spectral content of the remotely sensed data gained importance for the generation of the objects.

438 The fluctuating classification accuracy associated with pure training sometimes showed a peak
439 with segmentation settings which were near to optimal (e.g. point A in Figure 6c and point F in
440 Figure 6d). This may suggest that larger accuracy of the image segmentation analysis offers
441 larger classification accuracy and justifies the common practice for searching for optimal image
442 segmentation results (Dorren, 2003; Gao et al., 2011; Hirata and Takahashi, 2011; Kim et al.,
443 2009; Kim and Warner, 2011; Mishra and Crews, 2014). Indeed, since image segmentation and
444 object-based classification have become popular methods for land cover mapping, the body of
445 literature dedicated to methods for parameterization and accuracy assessment of image
446 segmentation has grown (Clinton et al., 2010; Whiteside et al., 2014; Yang et al., 2015).
447 Typically, these methods are focused on finding a segmentation result considered as being
448 optimal in the sense that over- and under-segmentation error are minimal and balanced.
449 However, a comprehensive analysis of the results shows that over-segmentation is associated
450 with larger classification accuracy, and thus the assessment of segmentation accuracy is not
451 necessarily informative for the prediction of an accuracy object-based classification (Figure 4 and
452 Figure 6; Li et al., 2016; Ma et al., 2015). A number of studies (Belgiu and Drăguț, 2014;
453 Räsänen et al., 2013; Verbeeck et al., 2012) have observed that classification accuracy and
454 segmentation accuracy, the latter at least as defined by empirical discrepancy methods, may not
455 be positively related.

456 It was notable that the results showed a positive trend of classification accuracy with over-
457 segmentation. In the situation of over-segmentation the size and spectral content of the objects
458 generated become close to those of the pixels, and thus the results suggest that classification
459 accuracy might possibly reach a maximum if per-pixel or near to per-pixel (Dronova et al., 2012;
460 Ju et al., 2005) classification had been undertaken. Comparing object-based and per-pixel image
461 classification has received much attention, and some publications have reported similar or larger
462 accuracy of per-pixel classification as compared to object-based classification (Cai and Liu,
463 2013; Goodin et al., 2015; Robertson and King, 2011). However, the majority of the literature
464 actually appears to hold the contrary view, that is that object-based classification achieves larger
465 accuracy than per-pixel (Estoque et al., 2015; Goodin et al., 2015; Memarian et al., 2013;
466 Whiteside et al., 2011). Apparently, the view that object-based classification is superior to per-
467 pixel classification has become widespread and commonly unquestionable. The results presented
468 above emphasize the need for more research in this respect. For example, typical comparisons
469 between object-based and per-pixel classifications have relied on pure training, while the use of
470 mixed training, which is also beneficial for per-pixel classification (Eastman and Laney, 2002;
471 Foody, 1997; Hansen, 2012; Zhang and Foody, 2001), should be considered in comparative
472 studies. Furthermore, it should be taken into account that the suitability of per-pixel and object-
473 based classifications may depend on scale issues related to the land cover patterns on the ground,
474 and the spatial resolution of the remotely sensed data and classification nomenclature used. For
475 example, the appropriateness of a segmentation level varies as a function of the land cover

476 classes mapped (Castilla et al., 2014; Kim and Warner, 2011; Laliberte and Rango, 2009) not
477 least because the definition of categorical classes is a scale dependent issue (Ju et al., 2005).

478 Finally, this study used an artificial neural network and generalized linear model able to
479 accommodate mixed objects which is a fundamental aspect to take into account if training using
480 impure units is to be undertaken. Alternative parametric classifiers, such as the maximum
481 likelihood classification provided in commonly used software packages, may be less appropriate
482 as relatively large and representative samples formed by pure training units are needed to
483 describe the classes; unless the training statistics are rectified. For example, the component parts
484 of a mixed object can be unmixed and used to estimate the signal of the object as it would be if
485 pure (Foody and Arora, 1996). The use of mixed objects for training a classification is, therefore,
486 possible for a range of classifiers and may facilitate land cover mapping from remote sensing.
487 The mixed nature of the spatial units used may also be addressed at the class allocation stage as
488 partial and multi class membership are estimated, which can then be assessed based, for example,
489 on the fuzzy confusion matrix (Binaghi et al., 1999; Stehman et al., 2007). This paper focused on
490 the training stage, but a fully fuzzy classification approach may be implemented for thematic
491 mapping (Foody, 1997; Zhang and Foody, 2001).

492 **5. Conclusions**

493 An implicit assumption made typically in object-based image classification is that the objects are
494 pure. This is often not the case, and in this paper it was shown that mixed objects can be
495 accommodated into the training stage of an object-based image classification. Contrary to

496 common practice, it may be, therefore, not necessary to remove mixed objects from the training
497 stage of a supervised image classification. Rather, an analysis of the effects of allowing mixed
498 objects in training should be considered, which also affords an increase in the size of the training
499 data set, and may contribute to an increase in classification accuracy. For example, by using
500 mixed objects in this study often the overall accuracy increased by around 25% relative to that
501 achieved using pure objects only. Furthermore, the results suggest that it may not be necessary to
502 follow common practice and seek an optimal segmentation output. Specifically, deliberate over-
503 segmentation may be a suitable strategy for generating objects for optimal training.

504 **Acknowledgements**

505 The authors are grateful to Markus Möller from the University of Halle (Saale) for providing R
506 code, the LISS-III data used was provided by the European Space Agency, and the research was
507 supported by the PhD Studentship SFRH/BD/77031/2011 from the “Fundação para a Ciência e
508 Tecnologia” (FCT), funded by the “Programa Operacional Potencial Humano” (POPH) and the
509 European Social Fund. The quality of the original manuscript was improved based on valuable
510 suggestions of anonymous reviewers and the Associate Editor.

511 **References**

- 512 Addink, E.A., Van Coillie, F.M.B., De Jong, S.M., 2012. Introduction to the GEOBIA 2010
513 special issue: From pixels to geographic objects in remote sensing image analysis. *Int. J.*
514 *Appl. Earth Obs. Geoinf.* 15, 1–6. doi:10.1016/j.jag.2011.12.001
- 515 Baatz, M., Schäpe, A., 2000. Multiresolution Segmentation: an optimization approach for high
516 quality multi-scale image segmentation, in: Strobl, J., Blaschke, T., Griesebner, G. (Eds.),
517 *Angewandte Geographische Informationsverarbeitung XII. Beiträge Zum AGIT-Symposium*

- 518 Salzburg 2000. Herbert Wichmann Verlag, Heidelberg, pp. 12–23.
- 519 Belgiu, M., Drăguț, L., 2014. Comparing supervised and unsupervised multiresolution
520 segmentation approaches for extracting buildings from very high resolution imagery. ISPRS
521 J. Photogramm. Remote Sens. 96, 67–75. doi:10.1016/j.isprsjprs.2014.07.002
- 522 Binaghi, E., Brivio, P.A., Ghezzi, P., Rampini, A., 1999. A fuzzy set-based accuracy assessment
523 of soft classification. Pattern Recognit. Lett. 20, 935–948. doi:10.1016/S0167-
524 8655(99)00061-6
- 525 Blaschke, T., Hay, G.J., Kelly, M., Lang, S., Hofmann, P., Addink, E.A., Queiroz Feitosa, R.,
526 van der Meer, F., van der Werff, H., van Coillie, F., Tiede, D., 2014. Geographic Object-
527 Based Image Analysis – Towards a new paradigm. ISPRS J. Photogramm. Remote Sens. 87,
528 180–191. doi:10.1016/j.isprsjprs.2013.09.014
- 529 Boyden, J., Joyce, K.E., Boggs, G., Wurm, P., 2013. Object-based mapping of native vegetation
530 and para grass (*Urochloa mutica*) on a monsoonal wetland of Kakadu NP using a Landsat 5
531 TM Dry-season time series. J. Spat. Sci. 58, 53–77. doi:10.1080/14498596.2012.759086
- 532 Caetano, M., Nunes, A., Dinis, J., Pereira, M. d. C., Marrecas, P., Nunes, V., 2010. Carta de uso
533 e ocupação do solo de Portugal Continental para 2007: Memória descritiva. Instituto
534 Geográfico Português, Lisbon.
- 535 Cai, S., Liu, D., 2013. A comparison of object-based and contextual pixel-based classifications
536 using high and medium spatial resolution images. Remote Sens. Lett. 4, 998–1007.
537 doi:10.1080/2150704X.2013.828180
- 538 Cánovas-García, F., Alonso-Sarría, F., 2015. A local approach to optimize the scale parameter in
539 multiresolution segmentation for multispectral imagery. Geocarto Int. 30, 937–961.
540 doi:10.1080/10106049.2015.1004131
- 541 Carrão, H., Goncalves, P., Caetano, M., 2008. Contribution of multispectral and multitemporal
542 information from MODIS images to land cover classification. Remote Sens. Environ. 112,
543 986–997. doi:10.1016/j.rse.2007.07.002
- 544 Castilla, G., Hernando, A., Zhang, C., McDermid, G.J., 2014. The impact of object size on the
545 thematic accuracy of landcover maps. Int. J. Remote Sens. 35, 1029–1037.
546 doi:10.1080/01431161.2013.875630
- 547 Clinton, N., Holt, A., Scarborough, J., Yan, L., Gong, P., 2010. Accuracy assessment measures
548 for object-based image segmentation goodness. Photogramm. Eng. Remote Sensing 76,
549 289–299.
- 550 Costa, H., Foody, G.M., Boyd, D.S., 2015. Integrating user needs on misclassification error

- 551 sensitivity into image segmentation quality assessment. *Photogramm. Eng. Remote Sensing*
552 81, 451–459. doi:10.14358/PERS.81.6.451
- 553 Cracknell, A.P., 1998. Synergy in remote sensing-what's in a pixel? *Int. J. Remote Sens.* 19,
554 2025–2047.
- 555 Dean, A.M., Smith, G.M., 2003. An evaluation of per-parcel land cover mapping using
556 maximum likelihood class probabilities. *Int. J. Remote Sens.* 24, 2905–2920.
557 doi:10.1080/01431160210155910
- 558 Dorren, L., 2003. Improved Landsat-based forest mapping in steep mountainous terrain using
559 object-based classification. *For. Ecol. Manage.* 183, 31–46. doi:10.1016/S0378-
560 1127(03)00113-0
- 561 Dronova, I., Gong, P., Clinton, N.E., Wang, L., Fu, W., Qi, S., Liu, Y., 2012. Landscape analysis
562 of wetland plant functional types: The effects of image segmentation scale, vegetation
563 classes and classification methods. *Remote Sens. Environ.* 127, 357–369.
564 doi:10.1016/j.rse.2012.09.018
- 565 Dronova, I., Gong, P., Wang, L., 2011. Object-based analysis and change detection of major
566 wetland cover types and their classification uncertainty during the low water period at
567 Poyang Lake, China. *Remote Sens. Environ.* 115, 3220–3236.
568 doi:10.1016/j.rse.2011.07.006
- 569 Eastman, J.R., Laney, R.M., 2002. Bayesian soft classification for sub-pixel analysis: a critical
570 evaluation. *Photogramm. Eng. Remote Sens.* 68, 1149–1154.
- 571 Ediriwickrema, J., Khorram, S., 1997. Hierarchical maximum-likelihood classification for
572 improved accuracies. *IEEE Trans. Geosci. Remote Sens.* 35, 810–816.
573 doi:10.1109/36.602523
- 574 Estoque, R.C., Murayama, Y., Akiyama, C.M., 2015. Pixel-based and object-based
575 classifications using high- and medium-spatial-resolution imageries in the urban and
576 suburban landscapes. *Geocarto Int.* 30, 1113–1129. doi:10.1080/10106049.2015.1027291
- 577 Fisher, P., 1997. The pixel: A snare and a delusion. *Int. J. Remote Sens.* 18, 679–685.
578 doi:10.1080/014311697219015
- 579 Foody, G.M., 2008. Harshness in image classification accuracy assessment. *Int. J. Remote Sens.*
580 29, 3137–3158. doi:10.1080/01431160701442120
- 581 Foody, G.M., 2000. Estimation of sub-pixel land cover composition in the presence of untrained
582 classes. *Comput. Geosci.* 26, 469–478. doi:10.1016/S0098-3004(99)00125-9

- 583 Foody, G.M., 1999a. The continuum of classification fuzziness in thematic mapping.
584 *Photogramm. Eng. Remote Sensing* 65, 443–451.
- 585 Foody, G.M., 1999b. The significance of border training patterns in classification by a
586 feedforward neural network using back propagation learning. *Int. J. Remote Sens.* 20, 3549–
587 3562. doi:10.1080/014311699211192
- 588 Foody, G.M., 1997. Fully fuzzy supervised classification of land cover from remotely sensed
589 imagery with an artificial neural network. *Neural Comput. Appl.* 5, 238–247.
590 doi:10.1007/BF01424229
- 591 Foody, G.M., 1996. Approaches for the production and evaluation of fuzzy land cover
592 classifications from remotely-sensed data. *Int. J. Remote Sens.* 17, 1317–1340.
593 doi:10.1080/01431169608948706
- 594 Foody, G.M., 1995. Cross-entropy for the evaluation of the accuracy of a fuzzy land cover
595 classification with fuzzy ground data. *ISPRS J. Photogramm. Remote Sens.* 50, 2–12.
596 doi:10.1016/0924-2716(95)90116-V
- 597 Foody, G.M., Arora, M.K., 1996. Incorporating mixed pixels in the training, allocation and
598 testing stages of supervised classifications. *Pattern Recognit. Lett.* 17, 1389–1398.
599 doi:10.1016/S0167-8655(96)00095-5
- 600 Foody, G.M., Mathur, A., 2006. The use of small training sets containing mixed pixels for
601 accurate hard image classification: Training on mixed spectral responses for classification
602 by a SVM. *Remote Sens. Environ.* 103, 179–189. doi:10.1016/j.rse.2006.04.001
- 603 Friedman, J., Hastie, T., Tibshirani, R., 2010. Regularization Paths for Generalized Linear
604 Models via Coordinate Descent. *J. Stat. Softw.* 33, 1–22. doi:10.1359/JBMR.0301229
- 605 Fritz, S., See, L., You, L., Justice, C., Becker-Reshef, I., Bydekerke, L., Cumani, R., Defourny,
606 P., Erb, K., Foley, J., Gilliams, S., Gong, P., Hansen, M., Hertel, T., Herold, M., Herrero,
607 M., Kayitakire, F., Latham, J., Leo, O., McCallum, I., Obersteiner, M., Ramankutty, N.,
608 Rocha, J., Tang, H., Thornton, P., Vancutsem, C., van der Velde, M., Wood, S., Woodcock,
609 C., 2013. The need for improved maps of global cropland. *Eos, Trans. Am. Geophys. Union*
610 94, 31–32. doi:10.1002/2013EO030006
- 611 Gao, Y., Mas, J.F., Kerle, N., Pacheco, J.A.N., 2011. Optimal region growing segmentation and
612 its effect on classification accuracy. *Int. J. Remote Sens.* 32, 3747–3763.
613 doi:10.1080/01431161003777189
- 614 Gardi, C., Panagos, P., Van Liedekerke, M., Bosco, C., De Brogniez, D., 2015. Land take and
615 food security: assessment of land take on the agricultural production in Europe. *J. Environ.*
616 *Plan. Manag.* 58, 898–912. doi:10.1080/09640568.2014.899490

- 617 Goodin, D.G., Anibas, K.L., Bezymennyi, M., 2015. Mapping land cover and land use from
618 object-based classification: An example from a complex agricultural landscape. *Int. J.*
619 *Remote Sens.* 36, 4702–4723. doi:10.1080/01431161.2015.1088674
- 620 Güttler, F.N., Ienco, D., Poncet, P., Teisseire, M., 2016. Combining transductive and active
621 learning to improve object-based classification of remote sensing images. *Remote Sens.*
622 *Lett.* 7, 358–367. doi:10.1080/2150704X.2016.1142678
- 623 Hagner, O., Reese, H., 2007. A method for calibrated maximum likelihood classification of
624 forest types. *Remote Sens. Environ.* 110, 438–444. doi:10.1016/j.rse.2006.08.017
- 625 Hansen, M., 2012. Classification trees and mixed pixel training data, in: *Remote Sensing of Land*
626 *Use and Land Cover, Remote Sensing Applications Series.* CRC Press, pp. 127–136.
627 doi:doi:10.1201/b11964-12
- 628 Heumann, B.W., 2011. An Object-Based Classification of Mangroves Using a Hybrid Decision
629 Tree—Support Vector Machine Approach. *Remote Sens.* 3, 2440–2460.
630 doi:10.3390/rs3112440
- 631 Hill, R., Granica, K., Smith, G.M., Schardt, M., 2007. Representation of an alpine treeline
632 ecotone in SPOT 5 HRG data. *Remote Sens. Environ.* 110, 458–467.
633 doi:10.1016/j.rse.2006.11.031
- 634 Hirata, Y., Takahashi, T., 2011. Image segmentation and classification of Landsat Thematic
635 Mapper data using a sampling approach for forest cover assessment. *Can. J. For. Res.* 41,
636 35–43. doi:10.1139/X10-130
- 637 Ju, J., Gopal, S., Kolaczyk, E.D., 2005. On the choice of spatial and categorical scale in remote
638 sensing land cover classification. *Remote Sens. Environ.* 96, 62–77.
639 doi:10.1016/j.rse.2005.01.016
- 640 Kim, M., Madden, M., Warner, T.A., 2009. Forest type mapping using object-specific texture
641 measures from multispectral Ikonos Imagery: Segmentation quality and image classification
642 issues. *Photogramm. Eng. Remote Sensing* 75, 819–829.
- 643 Kim, M., Warner, T., 2011. Multi-scale GEOBIA with very high spatial resolution digital aerial
644 imagery: scale, texture and image objects. *Int. J. Remote Sens.* 32, 2825–2850.
645 doi:10.1080/01431161003745608
- 646 Körting, T.S., Garcia Fonseca, L.M., Câmara, G., 2013. GeoDMA—Geographic Data Mining
647 Analyst. *Comput. Geosci.* 57, 133–145. doi:10.1016/j.cageo.2013.02.007
- 648 Laliberte, A.S., Rango, A., 2009. Texture and scale in object-based analysis of subdecimeter
649 resolution unmanned aerial vehicle (UAV) imagery. *IEEE Trans. Geosci. Remote Sens.* 47,

- 650 1–10. doi:10.1109/TGRS.2008.2009355
- 651 Lee, S., Lathrop, R.G., 2006. Subpixel analysis of landsat ETM + using Self-Organizing Map
652 (SOM) neural networks for urban land cover characterization. *IEEE Trans. Geosci. Remote*
653 *Sens.* 44, 1642–1654. doi:10.1109/TGRS.2006.869984
- 654 Li, M., Ma, L., Blaschke, T., Cheng, L., Tiede, D., 2016. A systematic comparison of different
655 object-based classification techniques using high spatial resolution imagery in agricultural
656 environments. *Int. J. Appl. Earth Obs. Geoinf.* 49, 87–98. doi:10.1016/j.jag.2016.01.011
- 657 Lu, D., Weng, Q., 2007. A survey of image classification methods and techniques for improving
658 classification performance. *Int. J. Remote Sens.* 28, 823–870.
659 doi:10.1080/01431160600746456
- 660 Luo, H., Wang, L., Shao, Z., Li, D., 2015. Development of a multi-scale object-based shadow
661 detection method for high spatial resolution image. *Remote Sens. Lett.* 6, 59–68.
662 doi:10.1080/2150704X.2014.1001079
- 663 Luysaert, S., Jammot, M., Stoy, P.C., Estel, S., Pongratz, J., Ceschia, E., Churkina, G., Don, A.,
664 Erb, K., Ferlicoq, M., Gielen, B., Grünwald, T., Houghton, R.A., Klumpp, K., Knohl, A.,
665 Kolb, T., Kuemmerle, T., Laurila, T., Lohila, A., Loustau, D., McGrath, M.J., Meyfroidt, P.,
666 Moors, E.J., Naudts, K., Novick, K., Otto, J., Pilegaard, K., Pio, C.A., Rambal, S.,
667 Rebmann, C., Ryder, J., Suyker, A.E., Varlagin, A., Wattenbach, M., Dolman, A.J., 2014.
668 Land management and land-cover change have impacts of similar magnitude on
669 surface temperature. *Nat. Clim. Chang.* 4, 389–393. doi:10.1038/nclimate2196
- 670 Ma, L., Cheng, L., Li, M., Liu, Y., Ma, X., 2015. Training set size, scale, and features in
671 Geographic Object-Based Image Analysis of very high resolution unmanned aerial vehicle
672 imagery. *ISPRS J. Photogramm. Remote Sens.* 102, 14–27.
673 doi:10.1016/j.isprsjprs.2014.12.026
- 674 Mahmood, R., Pielke, R.A., Hubbard, K.G., Niyogi, D., Dirmeyer, P.A., McAlpine, C., Carleton,
675 A.M., Hale, R., Gameda, S., Beltrán-Przekurat, A., Baker, B., McNider, R., Legates, D.R.,
676 Shepherd, M., Du, J., Blanken, P.D., Frauenfeld, O.W., Nair, U.S., Fall, S., 2014. Land
677 cover changes and their biogeophysical effects on climate. *Int. J. Climatol.* 34, 929–953.
678 doi:10.1002/joc.3736
- 679 Martin, Y., Van Dyck, H., Dendoncker, N., Titeux, N., 2013. Testing instead of assuming the
680 importance of land use change scenarios to model species distributions under climate
681 change. *Glob. Ecol. Biogeogr.* 22, 1204–1216. doi:10.1111/geb.12087
- 682 Memarian, H., Balasundram, S.K., Khosla, R., 2013. Comparison between pixel- and object-
683 based image classification of a tropical landscape using Système Pour l’Observation de la

- 684 Terre-5 imagery. *J. Appl. Remote Sens.* 7, 73512. doi:10.1117/1.JRS.7.073512
- 685 Millard, K., Richardson, M., 2015. On the importance of training data sample selection in
686 random forest image classification: a case study in peatland ecosystem mapping. *Remote*
687 *Sens.* doi:10.3390/rs70708489
- 688 Mishra, N.B., Crews, K. a., 2014. Mapping vegetation morphology types in a dry savanna
689 ecosystem: integrating hierarchical object-based image analysis with Random Forest. *Int. J.*
690 *Remote Sens.* 35, 1175–1198. doi:10.1080/01431161.2013.876120
- 691 Möller, M., Birger, J., Gidudu, A., Gläßer, C., 2013. A framework for the geometric accuracy
692 assessment of classified objects. *Int. J. Remote Sens.* 34, 8685–8698.
693 doi:10.1080/01431161.2013.845319
- 694 Momeni, R., Aplin, P., Boyd, D., 2016. Mapping complex urban land cover from spaceborne
695 imagery: The influence of spatial resolution, spectral band set and classification approach.
696 *Remote Sens.* 8, 88. doi:10.3390/rs8020088
- 697 Mui, A., He, Y., Weng, Q., 2015. An object-based approach to delineate wetlands across
698 landscapes of varied disturbance with high spatial resolution satellite imagery. *ISPRS J.*
699 *Photogramm. Remote Sens.* 109, 30–46. doi:10.1016/j.isprsjprs.2015.08.005
- 700 Müller, R., Krauß, T., Lehner, M., Reinartz, P., Forsgren, J., Rönnbäck, G., Karlsson, Å., 2009.
701 IMAGE 2006 European coverage, methodology and results.
- 702 Pal, M., Foody, G.M., 2012. Evaluation of SVM, RVM and SMLR for accurate image
703 classification with limited ground data. *IEEE J. Sel. Top. Appl. Earth Obs. Remote Sens.* 5,
704 1344–1355. doi:10.1109/JSTARS.2012.2215310
- 705 Paola, J.D., Schowengerdt, R. a., 1995. A detailed comparison of backpropagation neural
706 network and maximum-likelihood classifiers for urban land use classification. *IEEE Trans.*
707 *Geosci. Remote Sens.* 33, 981–996. doi:10.1109/36.406684
- 708 R Core Team, 2016. R: a language and environment for statistical computing.
- 709 Räsänen, A., Rusanen, A., Kuitunen, M., Lensu, A., 2013. What makes segmentation good? A
710 case study in boreal forest habitat mapping. *Int. J. Remote Sens.* 34, 8603–8627.
711 doi:10.1080/01431161.2013.845318
- 712 Richards, J., Kingsbury, N., 2014. Is there a preferred classifier for operational thematic
713 mapping? *IEEE Trans. Geosci. Remote Sens.* 52, 2715–2725.
714 doi:10.1109/TGRS.2013.2264831
- 715 Robertson, L.D., King, D.J., 2011. Comparison of pixel- and object-based classification in land

- 716 cover change mapping. *Int. J. Remote Sens.* 32, 1505–1529.
717 doi:10.1080/01431160903571791
- 718 Samat, A., Li, J., Liu, S., Du, P., Miao, Z., Luo, J., 2016. Improved hyperspectral image
719 classification by active learning using pre-designed mixed pixels. *Pattern Recognit.* 51, 43–
720 58. doi:10.1016/j.patcog.2015.08.019
- 721 Shimabukuro, Y.E., Miettinen, J., Beuchle, R., Grecchi, R.C., Simonetti, D., Achard, F., 2015.
722 Estimating burned area in Mato Grosso, Brazil, using an object-based classification method
723 on a systematic sample of medium resolution satellite images. *IEEE J. Sel. Top. Appl. Earth*
724 *Obs. Remote Sens.* 8, 4502–4508. doi:10.1109/JSTARS.2015.2464097
- 725 Stehman, S. V., Arora, M.K., Kasetkasem, T., Varshney, P.K., 2007. Estimation of fuzzy error
726 matrix accuracy measures under stratified random sampling. *Photogramm. Eng. Remote*
727 *Sensing* 73, 165–173. doi:10.14358/PERS.73.2.165
- 728 Tuanmu, M.-N., Jetz, W., 2014. A global 1-km consensus land-cover product for biodiversity
729 and ecosystem modelling. *Glob. Ecol. Biogeogr.* 23, 1031–1045. doi:10.1111/geb.12182
- 730 Uddin, K., Shrestha, H.L., Murthy, M.S.R., Bajracharya, B., Shrestha, B., Gilani, H., Pradhan, S.,
731 Dangol, B., 2015. Development of 2010 national land cover database for the Nepal. *J.*
732 *Environ. Manage.* 148, 82–90. doi:10.1016/j.jenvman.2014.07.047
- 733 Van Coillie, F.M.B., Verbeke, L.P.C., De Wulf, R.R., 2008. Semi-automated forest stand
734 delineation using wavelet based segmentation of very high resolution optical imagery, in:
735 *Object-Based Image Analysis: Spatial Concepts for Knowledge-Driven Remote Sensing*
736 *Applications*. pp. 237–256. doi:10.1007/978-3-540-77058-9_13
- 737 van de Vlag, D.E., Stein, A., 2007. Incorporating Uncertainty via Hierarchical Classification
738 Using Fuzzy Decision Trees. *IEEE Trans. Geosci. Remote Sens.* 45, 237–245.
739 doi:10.1109/TGRS.2006.885403
- 740 Venables, W.N., Ripley, B.D., 2002. *Modern Applied Statistics with S*. Springer, New York.
- 741 Verbeeck, K., Hermy, M., Van Orshoven, J., 2012. External geo-information in the segmentation
742 of VHR imagery improves the detection of imperviousness in urban neighborhoods. *Int. J.*
743 *Appl. Earth Obs. Geoinf.* 18, 428–435. doi:10.1016/j.jag.2012.03.015
- 744 Wang, F., 1990. Fuzzy supervised classification of remote sensing images. *IEEE Trans. Geosci.*
745 *Remote Sens.* 28, 194–201. doi:10.1109/36.46698
- 746 Wang, L., Sousa, W.P., Gong, P., 2004. Integration of object-based and pixel-based classification
747 for mapping mangroves with IKONOS imagery. *Int. J. Remote Sens.* 25, 5655–5668.
748 doi:10.1080/014311602331291215

- 749 Whiteside, T.G., Boggs, G.S., Maier, S.W., 2011. Comparing object-based and pixel-based
750 classifications for mapping savannas. *Int. J. Appl. Earth Obs. Geoinf.* 13, 884–893.
751 doi:10.1016/j.jag.2011.06.008
- 752 Whiteside, T.G., Maier, S.W., Boggs, G.S., 2014. Area-based and location-based validation of
753 classified image objects. *Int. J. Appl. Earth Obs. Geoinf.* 28, 117–130.
754 doi:10.1016/j.jag.2013.11.009
- 755 Wu, C., 2009. Quantifying high-resolution impervious surfaces using spectral mixture analysis.
756 *Int. J. Remote Sens.* 30, 2915–2932. doi:10.1080/01431160802558634
- 757 Yang, J., He, Y., Caspersen, J., Jones, T., 2015. A discrepancy measure for segmentation
758 evaluation from the perspective of object recognition. *ISPRS J. Photogramm. Remote Sens.*
759 101, 186–192. doi:10.1016/j.isprsjprs.2014.12.015
- 760 Zhang, J., Foody, G.M., 2001. Fully-fuzzy supervised classification of sub-urban land cover from
761 remotely sensed imagery: Statistical and artificial neural network approaches. *Int. J. Remote*
762 *Sens.* 22, 615–628. doi:10.1080/01431160050505883
- 763 Zhang, Y.J., 1996. A survey on evaluation methods for image segmentation. *Pattern Recognit.*
764 29, 1335–1346. doi:10.1016/0031-3203(95)00169-7
- 765 Zhou, W., Huang, G., Troy, A., Cadenasso, M.L., 2009. Object-based land cover classification of
766 shaded areas in high spatial resolution imagery of urban areas: A comparison study. *Remote*
767 *Sens. Environ.* 113, 1769–1777. doi:10.1016/j.rse.2009.04.007
- 768 Zhou, W., Troy, A., 2008. An object-oriented approach for analysing and characterizing urban
769 landscape at the parcel level. *Int. J. Remote Sens.* 29, 3119–3135.
770 doi:10.1080/01431160701469065
- 771 Zhu, Z., Bi, J., Pan, Y., Ganguly, S., Anav, A., Xu, L., Samanta, A., Piao, S., Nemani, R.R.,
772 Myneni, R.B., 2013. Global data sets of vegetation Leaf Area Index (LAI)_{3g} and Fraction of
773 Photosynthetically Active Radiation (FPAR)_{3g} derived from Global Inventory Modeling
774 and Mapping Studies (GIMMS) Normalized Difference Vegetation Index (NDVI)_{3g} for the
775 period 1981 to 2. *Remote Sens.* 5, 927. doi:10.3390/rs5020927
- 776
777

778 LIST OF FIGURE CAPTIONS

779 Figure 1. Location of the study area.

780 Figure 2. Data sets used: a) reference land cover map, COS2007, representing Artificial surfaces in red,
781 Agricultural areas in yellow, Forest and semi natural areas in green, Open spaces with little or no
782 vegetation in grey, and Wetlands and water bodies in blue; the square areas outlined in black are the
783 training areas randomly located for the estimation of object-based training statistics. b) LISS-III image
784 collected in Summer of 2006; RGB composition of data acquired in the near infrared, short wave infrared
785 and red bands respectively.

786 Figure 3. Segmentation results: a) Segmentation output produced with colour=75 and scale=10. b)
787 Segmentation output produced with colour=75 and scale=80.

788 Figure 4. Segmentation accuracy based on Costa et al.'s (2015) adaptation of Möller et al.'s (2013)
789 method. Dotted horizontal line corresponds to optimal accuracy.

790 Figure 5. Size of training data sets.

791 Figure 6. Classification accuracy as a function of the parameter scale with parameter colour set at 1, 25,
792 50, 75, and 99. The results obtained using the three reduced versions of the mixed training data sets are
793 identified as #1, #2, and #3. Panel a) to e) and f) to j) refer to the artificial neural network and
794 generalized linear model respectively.

795 Figure 7. Land cover maps obtained using the segmentation output produced with colour=50 and
796 scale=40, the artificial neural network, and different training strategies. a) Pure training (accuracy:
797 50.4%). b) Mixed training (accuracy: 69.0%). c) Mixed training with reduced samples #1 (accuracy:
798 61.5%). d) Mixed training with reduced samples #3 (accuracy: 65.8%). Colour legend as in Figure 2.